Acta Cryst. (1962). **15**, 894

Structures of the Intermediate Phases $Ni_{10}Zr_7$ and $Ni_{10}Hf_7$*

BY M. E. KIRKPATRICK,† J. F. SMITH AND W. L. LARSEN

Institute for Atomic Research and Departments of Chemistry and Mechanical Engineering, Iowa State University, Ames, Iowa, U.S.A.

(*Received* 3 *March* 1961 *and in revised form* 13 *July* 1961 *and* 6 *December* 1961)

The crystal structures of the intermediate phases $Ni_{10}Zr_7$ and $Ni_{10}Hf_7$ were determined from single crystal data. The phase $Ni_{10}Zr_7$ shows some solid solubility which produces a structural distortion with an attendant change in space group symmetry when the composition varies from that of stoichiometry. Lattice dimensions of

$$a_0 = 12{\cdot}386,\ b_0 = 9{\cdot}156,\ c_0 = 9{\cdot}211\ \text{Å}$$

were determined for the stoichiometric phase which has the space group symmetry C_{2v}^{17}–$C2ca$. The structure is distorted to produce space group symmetry D_{2h}^{15}–$Pbca$ when the composition of the phase becomes rich in zirconium with respect to stoichiometry. The room temperature lattice dimensions of the phase at maximum zirconium saturation were determined as

$$a_0 = 12{\cdot}497,\ b_0 = 9{\cdot}210,\ c_0 = 9{\cdot}325\ \text{Å}\ .$$

The nature of the zirconium solubility in this phase was deduced from a knowledge of the structural geometry and the interatomic distances as being a random substitution of zirconium atoms on certain nickel sites. Sufficient data were obtained for the stoichiometric $Ni_{10}Hf_7$ phase to show it to be isostructural with the stoichiometric $Ni_{10}Zr_7$ phase. Lattice dimensions of

$$a_0 = 12{\cdot}275,\ b_0 = 9{\cdot}078,\ c_0 = 9{\cdot}126\ \text{Å}$$

were determined for the stoichiometric $Ni_{10}Hf_7$ structure.

Introduction

The initial study of the nickel-rich portion of the nickel–zirconium phase diagram by Smith & Guard (1957) has indicated the existence of a compound near the composition Ni_5Zr_4. A recent study of this system by Kirkpatrick (1961) has shown that this phase exists over a region of composition with the maximum stability limits being of the order of 56·3 at.% to 58·9 at.% on the basis of metallographic data. In the present investigation single crystals from both extremes of composition were investigated. Consideration of lattice parameters, crystal symmetry, and density indicates that the stoichiometry should be $Ni_{10}Zr_7$; this reasoning will be discussed in more detail later in the paper. Crystals having the composition of the nickel-rich phase boundary will be referred to as stoichiometric while crystals saturated with zirconium will be referred to as zirconium-rich. The need for this distinction arises from the fact that dissolution of zirconium in the structure produces a distortion which affects the characteristic extinctions and space group symmetry. However, the actual atomic arrangements at both composition limits are nearly identical, and it is quite apparent that infinitesimal variations in zirconium content should lead continuously from one structure to the other.

Single crystals were obtained on the basis of Kirkpatrick's (1961) proposed phase diagram. Crystals of the zirconium-rich phase were isolated by electrolysis from a 45 wt.% nickel alloy which had been heat treated at 975 °C. for 50 hr. to augment phase equilibration and crystal growth. Single crystals of the stoichiometric phase were prepared from a 49·5 wt.% nickel alloy which was held at a temperature just above the eutectic isotherm (1060 °C.) for a sufficient length of time to allow gravitational separation of the liquid from a rigid network of primary crystals. In both cases the crystals occurred as elongated rectangular prisms and those used for gathering intensity data were chosen with dimensions of the order of $0{\cdot}04 \times 0{\cdot}04 \times 0{\cdot}10$ mm. Single crystals of the stoichiometric $Ni_{10}Hf_7$ phase were prepared by a method similar to that described for the stoichiometric $Ni_{10}Zr_7$ crystals.

Qualitative spectrographic analysis of representative crystals of zirconium-rich and stoichiometric compositions of the phase $Ni_{10}Zr_7$ revealed the presence of Cr, Cu, Fe and Si as trace impurities. The concentrations of these trace impurities in each of the crystals examined were not significantly different. A similar analysis of crystals of the $Ni_{10}Hf_7$ phase indicated only trace amounts of Cu, Fe, Mg and Si.

The computational methods used throughout the

* Contribution No. 995. Work was performed in the Ames Laboratory of the U.S. Atomic Energy Commission.

† Present address: Space Technology Laboratories Inc., 1 Space Park, Redondo Beach, California, U.S.A.

investigation and the data common to the structure determinations are noted at this point to avoid repetition. The Weissenberg intensity data were processed through the use of the Incor I program of Zalkin & Jones (1956) for the IBM-650 computer. The atomic scattering factors were those of Thomas & Umeda (1957). Precession data were corrected for Lorentz and polarization effects in the manner of Lu (1943). Patterson & Fourier projections were evaluated through the TDF-2 program for the IBM-650 computer by Fitzwater & Williams (1958). Refinement of structural parameters was carried out by the method of least squares utilizing the program for the IBM-650 by Senko & Templeton as modified by Fitzwater (1958).

Structure determinations

Symmetry and cell dimensions

For crystals of the stoichiometric phase, Weissenberg patterns were obtained with Cu $K\alpha$ radiation for the levels ($h0l$) through ($h4l$) and precession patterns were obtained with Mo $K\alpha$ radiation for ($0kl$) through ($5kl$) as well as ($hk0$) through ($hk3$). Corresponding data were accumulated for the zirconium-rich phase. In every case the reciprocal lattice patterns exhibited C_{2l} symmetry, and both the stoichiometric and zirconium-rich phases were assigned diffraction symmetry D_{2h}.

The general (hkl) reflections for crystals of the stoichiometric phase were observed only when $h+k=2n$; ($h0l$) reflections occurred only for $h+l=2n$; and ($hk0$) reflections appeared only if $h=2n$. These extinctions and the diffraction symmetry indicate the probable space group symmetry to be C_{2v}^{17}–$C2ca$ or D_{2h}^{18}–$Cmca$.

In contrast no characteristic extinctions were observed in the general (hkl) reflections for the zirconium-rich phase; however, ($0kl$) reflections occurred only with $k=2n$, ($h0l$) reflections occurred only with $l=2n$, and ($hk0$) reflections occurred only with $h=2n$. The diffraction symmetry and characteristic extinctions thus unequivocally indicate space group symmetry D_{2h}^{15}–$Pbca$.

Precision lattice constants were determined for both the stoichiometric and zirconium-rich phases. A back-reflection Weissenberg camera similar to that described by Buerger (1942) was used to obtain data for the precise determination of a_0 and c_0. The data were plotted against the Nelson–Riley (1941) function and the parameters were found by extrapolation to $\theta=90°$. The data for determination of b_0 were obtained with Mo $K\alpha$ radiation using layer line spacings of levels 2 through 10 of rotation patterns. A precision value for b_0 was obtained by plotting the data against $\cos^2\theta$ and extrapolating to $\theta=90°$. The b_0 dimensions obtained in this manner are inherently less accurate than those obtained by an extrapolation of back-reflection data. The cell dimensions are listed in Table 1.

Table 1. *Precision lattice parameters for crystals of the stoichiometric and zirconium-rich phase boundaries of* $Ni_{10}Zr_7$

Stoichiometric	Zirconium-rich
$a_0 = 12{\cdot}386 \pm 0{\cdot}006$ Å	$a_0 = 12{\cdot}497 \pm 0{\cdot}004$ Å
$b_0 = 9{\cdot}156 \pm 0{\cdot}008$	$b_0 = 9{\cdot}210 \pm 0{\cdot}008$
$c_0 = 9{\cdot}211 \pm 0{\cdot}005$	$c_0 = 9{\cdot}325 \pm 0{\cdot}002$

The experimental density of a massive alloy of stoichiometric composition was 7·78 g.cm.$^{-3}$. With the assumption of four formula weights of $Ni_{10}Zr_7$ per unit cell, the cell dimensions in Table 1 yield a theoretical density of 7·79 g.cm.$^{-3}$. The experimental value for the composition of the zirconium-poor phase boundary is 48·0 wt.% nickel (Kirkpatrick, 1961) while the composition of $Ni_{10}Zr_7$ is 47·89 wt.% nickel. Furthermore, the minimum multiplicity of atomic positions in either space group C_{2v}^{17}–$C2ca$ or D_{2h}^{18}–$Cmca$ is fourfold which corresponds to the choice of four formula weights per unit cell. The density, stoichiometry, and cell content are thus the basis for referring to the zirconium-poor phase boundary as the stoichiometric composition.

Kirkpatrick's (1961) value for the composition of the zirconium-rich phase boundary is near 45·5 wt.% nickel. This composition is approximately equivalent to the formula $Ni_{38}Zr_{30}$ and could readily be achieved by the substitutional replacement of two nickel atoms by zirconium atoms. A cell having the dimensions given in Table 1 for the zirconium-rich phase with a content of $Ni_{38}Zr_{30}$ has a theoretical density of 7·68 g.cm.$^{-3}$ which is in good agreement with an observed density of 7·67 g.cm.$^{-3}$ for a massive alloy of 45·3 wt.% nickel. The substitutional replacement of nickel atoms by zirconium would tend to expand the lattice because of the size difference and such expansion is consistent with the fact that the cell of the zirconium-rich phase is larger than that of the stoichiometric phase. The substitutional replacement must be to some degree random because the minimum multiplicity of the atomic sites in space group D_{2h}^{15}–$Pbca$ is fourfold and exact specification of the replacement sites would therefore necessitate some other symmetry.

Structure of the zirconium-rich phase

Chronologically, the structure of the zirconium-rich phase was the first to be completed. Intensity data for the zirconium-rich structure were determined for the ($h0l$) reflections from Weissenberg photographs and for the ($hk0$) and ($0kl$) reflections from precession photographs. For each class of reflections Mo $K\alpha$ radiation was used to obtain a series of exposures with variable time parameters. Numerical values for the intensities of 289 independent reflections were determined by visual comparison of the recorded reflections against a standard intensity scale prepared with a strong reflection from the crystal under investigation in the manner described by Buerger (1960).

The intensity data were used to construct the Patterson projections $P(x, y)$, $P(x, z)$, and $P(y, z)$. The Patterson projections revealed possible y and z positional parameters of approximately 4/40, 8/40, 10/40, 12/40, and 16/40 and possible x parameters of approximately 3/40, 7/40, 10/40, 13/40, and 17/40. In space group D_{2h}^{15}–*Pbca* only three atomic sets are available: two fourfold sets, both parameterless, and a general eightfold set. Thus the structure must be based upon the occupancy of one fourfold set and three eightfold sets by zirconium atoms and of five eightfold sets by nickel. No attempt was made in the initial structure determination to account for the substitution of two nickel atoms by zirconium atoms. Since all of the eightfold sets are general sets, the choice of the fourfold set is arbitrary, and the set with an atom at the origin was chosen to facilitate the derivation of a trial structure from the Patterson projections.

After several unsuccessful attempts, a suitable trial structure was derived which satisfactorily matched the Patterson projections, had reasonable interatomic spacings, and gave reasonable agreement between the calculated and observed structure factors. This structure was refined by the method of least squares to yield the following reliability indices:

$$R_1=\Sigma||F_o|-|F_c||/\Sigma|F_o|=0{\cdot}163 \quad \text{and}$$
$$R_2=\Sigma(|F_o|-|F_c|)^2/\Sigma F_o^2=0{\cdot}0330\,.$$

The reliability index R_2 was also calculated for each zone of data as $R_2(hk0)=0{\cdot}018$, $R_2(h0l)=0{\cdot}063$, and $R_2(0kl)=0{\cdot}017$. The refined positional parameters with their standard deviations, σ, and temperature factors, B_n, are given in Table 2. The calculated structure factors based on the refined structural parameters are compared with the observed structure factors in Table 3. The resulting electron density projections, $\varrho(x, y)$ and $\varrho(y, z)$, are shown in Figs. 1 and 2, respectively.

Structure of the stoichiometric phase

Intensity data for 170 independent reflections of classes $(h0l)$ and $(0kl)$ were accumulated in a manner completely analogous to that used for the zirconium-rich phase. Because the structure of the zirconium-rich phase was already known it was relatively easy to postulate closely related trial structures in both space groups D_{2h}^{18}–*Cmca* and C_{2v}^{17}–*C2ca*. The $(h0l)$ intensity data were used to distinguish between these trial structures. Refinement of the trial parameters in the centrosymmetric space group D_{2h}^{18}–*Cmca* produced a minimum reliability index of $R_1(h0l)=0{\cdot}399$, whereas the trial structure with C_{2v}^{17}–*C2ca* symmetry refined rather quickly to $R_1(h0l)=0{\cdot}186$. On this basis the latter structure was chosen as most probably correct, and refinement of the composite $(h0l)$ and $(0kl)$ data resulted in $R_1=0{\cdot}166$ and $R_2=0{\cdot}023$. The refined positional parameters with their standard deviations and temperature factors are listed in Table 4, and a comparison of the calculated and observed structure factors is shown in Table 5. The electron density projection, $\varrho(y, z)$, is shown in Fig. 3. It should be noted that the symmetry representation *C2ca* was not converted to the more conventional *Aba*2 representation because the former more readily facilitates comparison of the structure of the stoichiometric phase with the zirconium-rich phase.

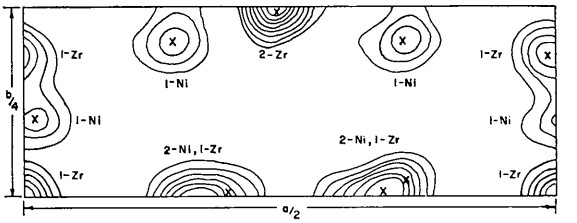

Fig. 1. Fourier projection, $\varrho(x, y)$, based on the refined structural parameters of the zirconium-rich $Ni_{10}Zr_7$ phase.

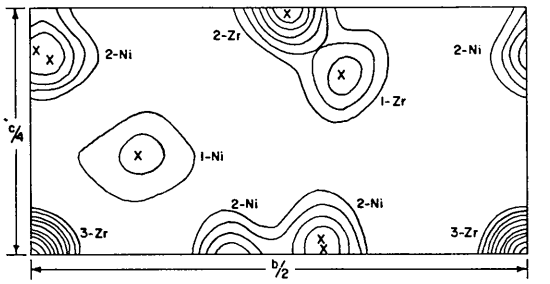

Fig. 2. Fourier projection, $\varrho(y, z)$, based on the refined structural parameters of the zirconium-rich $Ni_{10}Zr_7$ phase.

The structure of $Ni_{10}Hf_7$

A single crystal of $Ni_{10}Hf_7$ having a composition equal to that of the nickel-rich phase boundary was

Table 2. *Refined structural parameters for the zirconium-rich* $Ni_{10}Zr_7$ *phase*

Atom type	Wyckoff notation	x_n	y_n	z_n	$\sigma(x)$	$\sigma(y)$	$\sigma(z)$	B_n (Å^2)
Zr_0	4(*a*)	0	0	0	—	—	—	0·575
Zr_1	8(*c*)	0·3356	0·9983	0·9897	0·0008	0·0016	0·0013	1·227
Zr_2	8(*c*)	0·2378	0·2592	0·2440	0·0008	0·0014	0·0013	1·593
Zr_3	8(*c*)	0·4958	0·3156	0·3175	0·0009	0·0013	0·0012	1·280
Ni_4	8(*c*)	0·1950	0·0062	0·2080	0·0012	0·0018	0·0016	0·863
Ni_5	8(*c*)	0·3578	0·0196	0·2964	0·0010	0·0016	0·0014	0·475
Ni_6	8(*c*)	0·3557	0·2941	0·0042	0·0011	0·0017	0·0016	0·701
Ni_7	8(*c*)	0·6406	0·2917	0·0145	0·0010	0·0016	0·0014	0·520
Ni_8	8(*c*)	0·5083	0·1078	0·1023	0·0012	0·0018	0·0017	1·035

Table 3. *A comparison of observed and calculated structure factors for the refined zirconium-rich structure*

hkl	$\|F_o\|$	F_c	hkl	$\|F_o\|$	F_c	hkl	$\|F_o\|$	F_c	hkl	$\|F_o\|$	F_c
4,0,0	5.3	6.60	4,0,8	2.1	-1.98	5,0,16	2.6	-2.82	8,10,0	<1.9	3.28
6,0,0	25.3	26.67	5,0,8	<1.7	-0.86	6,0,16	<2.6	1.95	10,10,0	3.2	1.62
8,0,0	18.3	18.72	6,0,8	<1.8	1.11	2,1,0	<0.9	-0.94	2,11,0	<1.9	1.51
10,0,0	3.1	-2.24	7,0,8	<1.8	1.49	4,1,0	<1.2	1.98	4,11,0	<1.8	-0.90
12,0,0	9.7	10.38	8,0,8	2.7	3.78	6,1,0	<1.4	-3.03	6,11,0	<1.7	-1.82
14,0,0	11.6	11.40	9,0,8	<1.9	-2.49	8,1,0	4.0	4.05	8,11,0	<1.2	0.31
16,0,0	4.5	4.52	10,0,8	3.5	-6.75	10,1,0	2.6	-3.38	2,12,0	3.0	-1.46
18,0,0	3.3	-0.92	11,0,8	<2.1	-0.67	12,1,0	3.4	2.46	4,12,0	6.5	5.59
20,0,0	8.7	6.53	12,0,8	3.0	3.53	14,1,0	<2.0	-1.51	6,12,0	2.7	1.07
22,0,0	4.6	4.06	13,0,8	<2.2	0.44	16,1,0	2.7	2.13	0,2,0	<1.2	1.44
5,0,2	3.9	-2.24	14,0,8	<2.3	0.54	2,2,0	<1.1	0.55	0,2,1	<1.2	1.79
6,0,2	11.9	13.85	15,0,8	<2.4	-1.82	4,2,0	7.3	-6.96	0,2,2	2.9	5.24
7,0,2	<1.3	1.49	16,0,8	<2.4	-1.33	6,2,0	11.8	12.26	0,2,3	5.9	-5.24
8,0,2	<1.3	<0.10	17,0,8	<2.5	-0.30	8,2,0	9.5	-11.82	0,2,4	<1.5	-0.45
9,0,2	3.3	6.46	18,0,8	<2.6	0.66	10,2,0	7.4	5.67	0,2,5	<1.7	-0.35
10,0,2	7.1	-5.29	19,0,8	<2.6	-0.61	12,2,0	3.9	0.93	0,2,6	5.3	4.11
11,0,2	2.6	0.12	20,0,8	<2.7	0.31	14,2,0	2.0	-1.30	0,2,7	7.9	7.06
12,0,2	3.1	2.57	0,0,10	14.4	14.64	16,2,0	<1.9	-0.40	0,2,8	2.6	-3.02
13,0,2	2.6	1.17	1,0,10	2.3	1.08	2,3,0	<1.3	2.08	0,2,9	<2.2	1.62
14,0,2	3.0	3.73	2,0,10	4.0	4.22	4,3,0	2.8	-3.00	0,2,10	9.6	8.08
15,0,2	2.5	3.88	3,0,10	3.3	2.52	6,3,0	<1.6	-0.93	0,2,11	<2.2	-0.98
16,0,2	2.6	-3.57	4,0,10	4.1	-3.92	8,3,0	3.9	-3.63	0,2,12	4.1	-5.38
17,0,2	<2.2	1.55	5,0,10	4.8	-4.59	10,3,0	<1.9	2.40	0,4,0	24.4	26.99
18,0,2	<2.3	2.40	6,0,10	13.9	14.39	12,3,0	5.7	-5.59	0,4,1	12.3	-12.81
19,0,2	<2.4	1.38	7,0,10	3.5	0.83	14,3,0	<2.0	0.28	0,4,2	<1.5	-0.10
20,0,2	<2.2	<0.10	8,0,10	2.6	3.59	16,3,0	3.1	-2.43	0,4,3	3.5	2.02
0,0,4	24.7	27.02	9,0,10	<2.1	1.79	2,4,0	15.9	-16.79	0,4,4	27.4	25.03
1,0,4	5.4	4.02	10,0,10	<2.2	1.10	4,4,0	5.4	-5.46	0,4,5	<1.9	-0.61
2,0,4	18.1	-15.57	11,0,10	<2.3	-2.26	6,4,0	6.7	6.56	0,4,6	9.9	8.54
3,0,4	2.0	-4.44	12,0,10	<2.3	2.24	8,4,0	3.1	2.40	0,4,7	4.5	-5.33
4,0,4	6.0	-7.67	13,0,10	<2.4	-1.00	10,4,0	8.7	-7.78	0,4,8	7.6	7.45
5,0,4	<1.3	1.40	14,0,10	8.5	7.17	12,4,0	<2.0	2.72	0,4,9	3.2	1.51
6,0,4	5.5	6.61	15,0,10	<2.5	1.01	14,4,0	2.8	2.21	0,4,10	6.4	5.76
7,0,4	<1.4	2.57	16,0,10	<2.6	1.36	16,4,0	<1.6	0.16	0,4,11	3.0	-3.86
8,0,4	4.3	5.18	17,0,10	<2.6	-0.96	2,5,0	<1.7	0.41	0,4,12	2.5	2.68
9,0,4	2.8	-4.56	18,0,10	<2.7	-0.79	4,5,0	<1.7	1.63	0,6,0	12.3	12.94
10,0,4	8.3	-10.51	19,0,10	<2.7	-0.30	6,5,0	3.6	-4.33	0,6,1	3.7	3.82
11,0,4	<1.8	1.20	20,0,10	5.3	3.67	8,5,0	2.6	3.63	0,6,2	4.2	4.55
12,0,4	2.3	3.05	0,0,12	5.1	5.56	10,5,0	1.9	-1.61	0,6,3	3.2	3.49
13,0,4	<1.9	1.43	1,0,12	4.2	4.23	12,5,0	<2.0	0.40	0,6,4	5.8	7.35
14,0,4	3.5	3.39	2,0,12	2.6	1.27	14,5,0	<2.0	-1.79	0,6,5	<2.1	1.20
15,0,4	<2.1	-2.28	3,0,12	2.6	0.64	16,5,0	2.4	2.36	0,6,6	13.7	14.48
16,0,4	<2.2	-0.66	4,0,12	4.6	2.50	2,6,0	3.1	3.80	0,6,7	<2.2	0.22
17,0,4	<1.4	<0.10	5,0,12	<2.2	-1.87	4,6,0	5.4	-4.76	0,6,8	3.2	-3.28
18,0,4	5.1	-2.38	6,0,12	<2.2	2.32	6,6,0	16.8	16.21	0,6,9	<2.2	2.75
19,0,4	<1.1	<0.10	7,0,12	<2.3	1.20	8,6,0	<2.0	-1.64	0,6,10	9.0	9.28
20,0,4	5.5	2.64	8,0,12	3.3	4.89	10,6,0	5.5	3.83	0,8,0	7.7	9.40
0,0,6	12.6	13.07	9,0,12	<2.3	3.58	12,6,0	<2.0	2.86	0,8,1	5.3	-3.77
1,0,6	<1.3	1.20	10,9,12	<2.4	-1.63	14,6,0	5.3	4.44	0,8,2	<2.2	-1.01
2,0,6	2.7	5.70	11,0,12	<2.5	-0.87	2,7,0	2.6	3.35	0,8,3	4.4	4.82
3,0,6	2.5	5.46	12,0,12	3.6	4.42	4,7,0	<1.9	-0.27	0,8,4	5.4	7.02
4,0,6	7.7	-9.73	13,0,12	<2.6	0.84	6,7,0	<2.0	0.35	0,8,5	2.7	-3.82
5,0,6	4.7	-7.14	14,0,12	<2.6	1.50	8,7,0	<2.0	2.00	0,8,6	3.5	-3.70
6,0,6	17.6	16.81	0,0,14	2.9	2.61	10,7,0	5.0	5.08	0,8,7	<2.2	-2.86
7,0,6	2.6	-0.75	1,0,14	<2.4	0.96	12,7,0	<2.0	-2.22	0,8,8	6.1	5.39
8,0,6	2.3	3.07	2,0,14	<2.4	-2.45	14,7,0	4.7	3.89	0,8,9	<1.9	-1.70
9,0,6	2.7	6.13	3,0,14	<2.4	0.35	2,8,0	7.8	-7.33	0,8,10	<1.7	2.61
10,0,6	3.2	-1.29	4,0,14	5.9	-5.75	4,8,0	3.4	3.13	0,10,0	15.2	14.54
11,0,6	<1.9	-4.13	5,0,14	4.2	-1.60	6,8,0	<2.0	1.44	0,10,1	4.4	-4.71
12,0,6	<2.0	2.92	6,0,14	4.3	3.13	8,8,0	<2.0	-1.94	0,10,2	9.7	8.96
13,0,6	<2.1	-2.06	7,0,14	<2.5	2.04	10,8,0	<2.0	-0.20	0,10,3	2.2	0.82
14,0,6	6.4	7.07	8,0,14	<2.5	-1.68	12,8,0	<1.8	3.19	0,10,4	5.3	6.31
15,0,6	<2.2	2.85	9,0,14	<2.6	-1.10	2,9,0	<2.0	0.98	0,10,5	3.3	2.69
16,0,6	<2.3	-0.32	10,0,14	<2.6	-2.10	4,9,0	<2.0	0.97	0,10,6	10.0	9.78
17,0,6	<2.4	-0.93	11,0,14	<2.6	0.22	6,9,0	4.0	-4.18	0,10,7	3.4	-2.74
18,0,6	<2.5	0.78	12,0,14	<2.6	-1.40	8,9,0	<2.0	2.41	0,10,8	2.3	3.04
19,0,6	<2.5	-0.59	0,0,16	4.5	3.89	10,9,0	<1.9	-0.11	0,12,0	3.8	3.62
20,0,6	3.9	2.85	1,0,16	<2.6	2.48	12,9,0	<1.3	-1.20	0,12,1	3.2	-3.13
0,0,8	7.9	9.06	2,0,16	<2.6	0.54	2,10,0	3.4	3.82	0,12,2	3.6	-3.69
1,0,8	4.6	4.81	3,0,16	<2.6	0.94	4,10,0	4.4	-2.86	0,12,3	<2.1	1.02
2,0,8	7.3	-5.67	4,0,16	<2.6	0.80	6,10,0	15.7	14.02	0,12,4	4.0	2.60
3,0,8	2.3	-2.99							0,12,5	3.9	-2.54

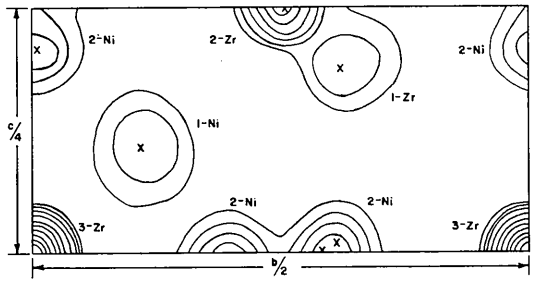

Fig. 3. Fourier projection, $\varrho(y, z)$, based on the refined structural parameters of the stoichiometric $Ni_{10}Zr_7$ phase.

obtained. This needle-shaped crystal was oriented with the needle-axis (b-axis) parallel to the axis of rotation. Extrapolation methods already described were utilized to determine the cell dimensions:

$$a_0 = 12{\cdot}275 \pm 0{\cdot}004,\ b_0 = 9{\cdot}078 \pm 0{\cdot}008,$$
$$c_0 = 9{\cdot}126 \pm 0{\cdot}005\ \text{Å}.$$

These cell dimensions with four formula weights of $Ni_{10}Hf_7$ indicate a theoretical density of 11·97 g.cm.$^{-3}$ which is in good agreement with an observed density of 11·96 g.cm.$^{-3}$ for a massive alloy of stoichiometric composition.

The diffraction symmetry and characteristic extinctions exhibited by this crystal were identical to those observed from the stoichiometric $Ni_{10}Zr_7$ phase. The correspondence of cell dimensions and symmetry data between $Ni_{10}Hf_7$ and $Ni_{10}Zr_7$ plus the close correspondence in atomic size and chemical behavior of hafnium and zirconium warranted an examination of intensity data from $Ni_{10}Hf_7$ to determine whether it was isostructural with $Ni_{10}Zr_7$. A comparison of observed intensities and calculated structure factors is shown in Table 6, and, while the observed intensities are only semiquantitative, the agreement is adequate to demonstrate that $Ni_{10}Hf_7$ is isostructural with the corresponding zirconium phase.

Results and discussion

A tabulation of the interatomic spacings about each type of atom in the structure is shown in Table 7 for both the stoichiometric and zirconium-rich compositions. The eightfold Zr_1 set of the zirconium-rich structure degenerates into two fourfold sets at the stoichiometric composition. In Table 7 these two fourfold sets are labeled Zr_{1a} and Zr_{1b}. The coordinated atoms form complete but irregular polyhedra, and the cut-off in tabulation is such that the omitted next nearest neighbor distance about any given atom is $\sim 0{\cdot}4$ Å or more greater than the largest tabulated distance to the same type of neighbor. From Tables 2, 4 and 7 it is quite apparent that the atomic arrangement is basically the same for both composition limits and differs only in the symmetry distortion which accompanies the substitutional replacement of nickel atoms by zirconium atoms. Indeed a continuous variation between the two composition limits by infinitesimal increments is readily possible. On the basis of the data in Table 7, the average coordination number is 12·4 which is indicative of a space-filling which is slightly more efficient than in the elemental structures. On this basis, atomic size considerations may be one of the factors relevant to phase stability.

The $Ni_{10}Zr_7$ structure is closely related to the NiZr structure (Kirkpatrick, Bailey & Smith, 1961) which is of the B_f type (Pearson, 1958). Both structures can be viewed as consisting of alternating layers of nickel atoms and of zirconium atoms. In both cases the layering may be observed in two independent directions. In $Ni_{10}Zr_7$ the layered planes are (011) and (01$\bar{1}$) while in NiZr the layered planes are (021) and (02$\bar{1}$). The lines of intersection of the layers are parallel to the respective a-parameter, and both structures are pseudo-tetragonal about this symmetry axis.

The layering in the $Ni_{10}Zr_7$ structure contrasts with that in the NiZr structure in at least two aspects. First, the zirconium layers of the $Ni_{10}Zr_7$ structure contain some nickel atoms while the layers in NiZr are exclusively of one species or the other. The nickel atoms in question are the Ni_8 atoms of the $Ni_{10}Zr_7$ structure and these atoms are presumably responsible for the second contrast. Since the nickel atoms are significantly smaller than the zirconium atoms, the area of the zirconium layers in $Ni_{10}Zr_7$ is contracted in comparison to the layers in NiZr and there is an attendant buckling or corrugation in the adjacent nickel layers. Thus the atoms in the nickel layers are much less coplanar in the $Ni_{10}Zr_7$ structures than in the NiZr structure.

Table 4. *Refined structural parameters for the stoichiometric* $Ni_{10}Zr_7$ *phase*

Atom type	Wyckoff notation	x_n	y_n	z_n	$\sigma(x)$	$\sigma(y)$	$\sigma(z)$	B_n (Å^2)
Zr_0	4(a)	0·0455	0	0	0·0019	—	—	0·816
Zr_{1a}	4(a)	0·3566	0	0	0·0014	—	—	0·801
Zr_{1b}	4(a)	0·7428	0	0	0·0011	—	—	0·451
Zr_2	8(b)	0·2982	0·2560	0·2459	0·0011	0·0012	0·0036	1·158
Zr_3	8(b)	0·5471	0·3106	0·3129	0·0016	0·0016	0·0010	1·041
Ni_4	8(b)	0·2418	0·0008	0·2100	0·0015	0·0008	0·0008	2·515
Ni_5	8(b)	0·4044	0·0082	0·2915	0·0009	0·0019	0·0009	0·503
Ni_6	8(b)	0·4022	0·2919	0·0031	0·0010	0·0020	0·0020	0·504
Ni_7	8(b)	0·6918	0·2986	0·0122	0·0012	0·0024	0·0014	0·696
Ni_8	8(b)	0·5499	0·1090	0·1063	0·0018	0·0021	0·0013	0·699

Table 5. *A comparison of observed and calculated structure factors for the refined stoichiometric* $Ni_{10}Zr_7$ *structure*

hkl	$\|F_o\|$	$\|F_c\|$	A_c	B_c	hkl	$\|F_o\|$	$\|F_c\|$	A_c	B_c	hkl	$\|F_o\|$	F_c
800	16.1	17.32	-8.72	14.96	12,0,8	1.2	1.42	-1.41	0.09	004	28.4	28.64
10,0,0	2.5	3.76	-3.02	2.24	14,0,8	2.3	0.65	-0.07	0.65	006	11.5	12.38
12,0,0	8.1	10.35	-6.18	-8.31	16,0,8	3.1	2.90	1.29	-2.60	008	11.8	12.29
14,0,0	12.8	10.67	-7.20	-7.88	18,0,8	4.6	4.71	-3.28	3.39	0,0,10	15.8	15.35
16,0,0	9.5	9.98	0.03	-9.97	20,0,8	3.2	3.74	3.56	-1.16	0,0,12	6.4	7.17
18,0,0	5.1	4.85	2.63	4.09	22,0,8	0.9	0.55	-0.54	0.09	0,0,14	3.3	3.44
20,0,0	13.7	11.23	11.03	-2.16	24,0,8	1.0	1.10	-0.65	-0.88	0,0,16	6.3	6.24
22,0,0	5.3	3.90	3.89	0.25	2,0,10	4.2	4.87	4.82	0.66	0,0,18	3.6	2.87
24,0,0	1.5	1.04	0.29	-1.00	4,0,10	1.9	1.77	-0.76	-1.60	0,0,20	5.9	4.29
26,0,0	4.3	3.30	-1.44	2.97	6,0,10	14.7	15.71	-6.69	14.21	022	5.6	5.91
602	11.4	13.13	2.94	12.79	8,0,10	3.1	3.58	0.52	3.54	023	6.2	-6.30
802	7.1	7.10	3.17	-6.35	10,0,10	4.3	5.81	-5.59	1.56	024	0.2	-0.21
10,0,2	6.2	4.45	-3.86	-2.20	12,0,10	0.8	2.70	0.84	-2.56	025	0.2	0.17
12,0,2	4.1	6.38	2.66	5.80	14,0,10	10.9	8.96	-5.29	-7.23	026	4.8	4.34
14,0,2	3.5	4.92	-1.97	-4.50	16,0,10	1.6	2.68	-0.86	-2.54	027	7.4	6.93
16,0,2	1.1	2.40	1.51	1.86	18,0,10	0.9	1.04	0.07	1.04	028	0.7	-0.88
18,0,2	0.8	1.69	-1.63	0.42	20,0,10	4.2	4.78	4.75	-0.57	029	0.3	-0.51
20,0,2	0.9	1.43	0.82	-1.17	22,0,10	5.6	3.80	3.77	0.44	0,2,10	6.2	7.43
22,0,2	1.7	1.79	1.34	1.19	2,0,12	3.9	3.32	-3.07	-1.26	0,2,11	0.2	-0.87
24,0,2	3.2	2.98	-1.84	-2.35	4,0,12	5.1	2.90	0.98	2.73	0,2,12	2.5	-3.67
26,0,2	2.8	2.40	0.38	2.36	6,0,12	0.8	1.77	1.23	1.27	041	11.6	-10.12
204	17.4	18.07	-14.07	-11.34	8,0,12	0.8	1.48	-1.38	0.55	042	0.2	-1.27
404	5.1	3.04	0.06	-3.04	10,0,12	1.3	0.70	-0.18	0.67	043	0.3	1.72
604	4.0	5.34	-3.80	3.76	12,0,12	3.0	2.19	-2.15	0.38	044	25.6	26.08
804	4.5	4.30	0.21	4.29	14,0,12	2.2	0.67	-0.24	0.62	045	0.2	0.45
10,0,4	8.6	6.68	6.67	0.28	16,0,12	3.8	2.81	1.14	-2.57	046	8.4	8.03
12,0,4	0.8	1.78	0.45	-1.72	18,0,12	1.9	2.26	-1.90	1.22	047	3.1	-3.62
14,0,4	2.4	2.54	-2.54	-0.01	20,0,12	2.7	2.72	2.36	-1.33	048	6.7	8.69
16,0,4	3.0	3.14	-0.49	-3.10	2,0,14	4.3	3.97	-1.71	-3.58	049	0.4	2.33
18,0,4	7.5	8.38	-5.63	6.20	4,0,14	7.7	6.53	-2.64	-5.97	0,4,10	5.5	5.48
20,0,4	6.5	5.63	5.42	-1.54	6,0,14	5.0	4.48	-3.09	3.24	0,4,11	2.0	-2.84
22,0,4	0.9	1.08	0.16	-1.06	8,0,14	3.6	4.42	4.37	-0.62	0,4,12	4.6	5.46
24,0,4	2.7	2.93	-0.88	-2.79	10,0,14	1.4	1.34	1.13	0.73	060	14.1	13.18
26,0,4	1.0	0.87	0.64	0.60	12,0,14	4.8	4.24	4.24	-0.07	061	4.7	6.30
28,0,4	2.2	1.41	0.06	1.40	14,0,14	3.6	2.32	-1.93	-1.28	062	5.4	6.04
206	2.5	3.90	3.58	1.54	16,0,14	2.8	1.92	-1.42	1.28	063	1.6	1.47
406	6.8	6.46	-2.38	-6.00	18,0,14	4.3	3.45	-1.90	2.88	064	9.4	8.90
606	15.6	15.69	-3.57	15.28	2,0,16	1.4	0.97	-0.64	-0.73	065	0.2	-0.33
806	1.9	2.51	2.50	0.19	4,0,16	4.1	2.56	0.93	2.38	066	14.3	14.66
10,0,6	4.7	5.34	-5.28	0.74	6,0,16	1.4	2.37	-0.64	2.28	067	0.2	0.40
12,0,6	2.0	2.40	1.92	1.43	8,0,16	1.5	1.70	-0.80	1.50	068	1.6	-1.87
14,0,6	8.3	7.76	-4.79	-6.11	10,0,16	0.9	1.23	-1.21	0.22	069	0.3	-0.54
16,0,6	0.8	0.63	-0.31	-0.55	12,0,16	2.9	1.67	-1.46	-0.82	0,6,10	11.0	10.70
18,0,6	0.8	1.58	-1.37	0.78	14,0,16	1.0	1.09	-1.01	-0.40	080	11.5	10.34
20,0,6	2.6	3.20	2.89	-1.35	16,0,16	2.3	2.37	0.26	-2.36	081	1.0	-1.64
22,0,6	4.5	2.84	2.81	0.37	2,0,18	0.9	0.71	0.43	-0.56	082	0.5	-1.83
24,0,6	3.5	2.93	-1.06	-2.73	4,0,18	1.5	0.98	-0.51	-0.84	083	3.6	3.94
26,0,6	3.6	2.60	-0.18	2.60	6,0,18	3.5	3.35	-1.69	2.90	084	6.0	7.34
208	8.4	8.60	-7.30	-4.56	8,0,18	1.8	1.30	1.30	0.08	085	1.1	-2.03
408	2.1	0.99	-0.16	0.97	10,0,18	2.0	1.57	-1.53	0.34	086	3.1	-4.19
608	0.8	1.25	0.93	0.82	12,0,18	1.5	1.13	0.98	-0.57	087	0.9	-1.82
808	0.6	1.74	0.35	0.88	2,0,20	1.5	1.43	-0.17	-1.43	088	7.1	7.51
10,0,8	2.0	3.34	3.04	-1.39	4,0,20	1.0	0.68	-0.09	0.67	0,10,0	16.5	16.22
										0,10,1	2.6	-2.86
										0,10,2	8.8	8.90
										0,10,3	0.4	-0.69
										0,10,4	5.4	6.88
										0,10,5	0.3	1.66
										0,10,6	12.6	11.55

Table 6. *A comparison of some observed intensity* data and calculated structure factors for the stoichiometric* $Ni_{10}Hf_7$ *phase*

hkl	$\|F_c\|$	Observed Intensity	hkl	$\|F_c\|$	Observed Intensity	hkl	$\|F_c\|$	Observed Intensity
400	28.2	vs	113	14.2	m	028	3.8	vw
600	26.5	vs	313	10.9	s	228	5.7	m
800	17.9	s	513	8.4	w	428	6.2	no
10,0,0	5.8	vw	713	6.5	w	628	6.6	m
12,0,0	7.2	w	913	5.6	w	828	3.9	no
14,0,0	5.7	w	114	5.5	w	0,2,10	5.6	w
002	0.8	no	314	16.9	s	2,2,10	3.8	w
202	3.5	no	514	3.4	w	4,2,10	3.1	vw
402	16.5	m	714	10.0	m	240	21.3	vs
602	16.8	m	914	4.6	w	440	6.6	w
802	12.7	m	115	8.0	w	640	6.0	vw
10,0,2	7.7	w	315	9.4	w	840	4.4	vw
12,0,2	4.6	w	515	8.1	w	10,4,0	1.5	no
14,0,2	2.3	no	715	5.2	w	041	14.1	m
004	38.4	vs	116	5.3	w	241	9.1	w
204	21.5	s	316	12.9	m	441	9.8	w
404	4.1	vw	516	1.7	no	641	6.9	w
604	5.5	vw	716	9.7	w	841	6.6	w
804	3.7	vw	117	7.2	w	10,4,1	2.9	no
10,0,4	1.9	vw	317	4.7	no	042	3.9	vw
12,0,4	1.6	vw	517	3.4	no	242	6.7	w
14,0,4	1.9	no	118	2.3	w	442	3.0	no
006	15.7	s	318	3.5	no	642	13.7	s
206	5.7	w	518	5.4	no	842	8.7	m
406	2.9	vw	220	2.8	no	10,4,2	9.7	m
606	16.5	s	420	8.6	m	043	3.5	no
806	3.4	vw	620	14.4	s	243	1.7	no
10,0,6	6.4	m	820	17.6	s	443	2.9	no
12,0,6	1.4	no	10,2,0	12.0	m	643	0.9	no
008	12.1	m	12,2,0	5.3	w	843	1.8	no
208	9.3	m	221	4.9	w	044	29.5	vs
408	1.8	vw	421	6.1	m	244	9.1	m
608	1.5	vw	621	3.1	vw	444	10.1	m
808	1.3	no	821	3.0	vw	644	7.0	w
10,0,8	0.6	no	022	25.5	s	844	3.8	vw
0,0,10	10.1	m	222	4.6	w	045	1.1	no
2,0,10	2.2	vw	422	34.1	vs	245	3.9	no
4,0,10	0.3	no	622	3.6	no	445	2.4	no
6,0,10	8.2	m	822	2.2	vw	645	2.2	no
8,0,10	1.8	no	223	6.4	w	845	0.9	no
111	23.7	s	423	7.4	m	046	9.2	m
311	20.0	s	623	4.0	vw	246	3.3	w
511	16.4	s	823	3.8	w	446	0.9	no
711	12.0	m	024	3.2	no	646	10.8	m
911	8.2	w	224	5.9	m	047	3.4	no
11,1,1	5.1	vw	424	1.8	no	247	3.5	no
112	7.8	w	624	12.6	s	447	1.7	no
312	11.1	m	824	10.5	m	647	3.0	no
512	13.4	m	026	10.2	m	847	1.7	no
712	13.4	m	226	11.2	m	048	9.3	m
912	1.2	no	426	10.1	m	248	5.5	w
11,1,2	5.6	vw	626	2.9	no	448	3.8	vw

* *vs*: very strong, *s*: strong, *m*: medium, *w*: weak, *vw*: very weak, *no*: not observed.

Table 7. *A comparison of interatomic distances in the zirconium-rich and stoichiometric* $Ni_{10}Zr_7$ *structures*

		Zr-rich Structure		Stoichiometric Structure	
Atom	Neighbor	No. of Neighbors	Distance, Å	No. of Neighbors	Distance, Å
Zr_o	Zr_3	2	3.37	2	3.36
		2	3.41	2	3.33
	Ni_4	2	3.11	2	3.11
	Ni_5	2	2.61	2	2.60
	Ni_6	2	2.62	2	2.60
	Ni_7	2	2.60	2	2.59
				(Atom-Zr_{1a})	(Atom-Zr_{1b})
Zr_1	Zr_2	1	3.59	2 3.34	2 3.25
		2	3.42	2 3.32	2 3.38
		1	3.36		
	Zr_3	1	3.24	2 3.40	2 3.44
		1	3.09		
	Ni_4	1	2.69	2 2.40	2 2.67
		1	2.65		
	Ni_5	1	2.88	2 2.75	2 2.77
		1	3.02		
	Ni_6	1	2.74	2 2.73	2 2.74
		1	3.04		
	Ni_7	1	3.11	2 2.75	2 2.81
		1	2.69		
	Ni_8	1	2.60	2 2.77	2 2.77
		1	2.34		
Zr_2	Zr_1	1	3.59	1	3.34
		2	3.42	1	3.32
		-	--	1	3.25
		1	3.36	1	3.38
	Zr_3	1	3.34	1	3.18
		1	3.12	1	3.20
	Ni_4	1	2.41	1	2.47
		1	2.45	1	2.38
	Ni_5	2	2.72	2	2.67
	Ni_6	1	2.70	1	2.65
		1	2.88	1	2.68
	Ni_7	1	2.74	1	2.76
		1	2.58	1	2.61
Zr_3	Zr_o	1	3.37	1	3.36
		1	3.41	1	3.33
	Zr_1	1	3.24	1	3.40
		1	3.09	1	3.44
	Zr_2	1	3.34	1	3.18
		1	3.12	1	3.20
	Ni_4	1	3.13	1	3.12
	Ni_5	1	3.23	1	3.29
		1	2.83	1	2.71
	Ni_6	1	2.67	1	2.64
		1	3.41	1	3.42
	Ni_7	1	2.76	1	2.75
		1	3.36	1	3.30
	Ni_8	1	2.79	1	2.83
		1	2.78	1	2.80
		1	2.75	1	2.65
Ni_4	Zr_o	1	3.11	1	3.11
	Zr_1	1	2.69	1	2.40
		1	2.65	1	2.67

		Zr-rich Structure		Stoichiometric Structure	
Atom	Neighbor	No. of Neighbors	Distance, Å	No. of Neighbors	Distance, Å
Ni_4	Zr_2	1	2.45	1	2.46
		1	2.41	1	2.37
	Zr_3	1	3.13	1	3.12
	Ni_5	1	2.20	1	2.15
	Ni_6	1	2.80	-	--
	Ni_7	1	2.87	1	2.82
		-	--	1	2.66
	Ni_8	1	3.07	1	3.08
Ni_5	Zr_o	1	2.61	1	2.60
	Zr_1	1	2.88	1	2.75
		1	3.02	1	2.77
	Zr_2	1	2.71	1	2.66
		1	2.72	1	2.68
	Zr_3	1	3.23	1	3.29
		1	2.83	1	2.71
	Ni_4	1	2.20	1	2.15
	Ni_6	1	2.59	1	2.63
		-	--	1	2.78
	Ni_7	1	2.74	-	--
	Ni_8	1	2.73	1	2.65
Ni_6	Zr_o	1	2.62	1	2.60
	Zr_1	1	2.74	1	2.73
		1	3.04	1	2.74
	Zr_2	1	2.88	1	2.65
		1	2.70	1	2.68
	Zr_3	1	2.67	1	2.64
		1	3.41	1	3.42
	Ni_4	1	2.80	-	--
	Ni_5	1	2.59	1	2.63
		-	--	1	2.78
	Ni_7	1	2.81	1	2.74
	Ni_8	1	2.72	1	2.68
Ni_7	Zr_o	1	2.60	1	2.58
	Zr_1	1	3.11	1	2.81
		1	2.69	1	2.75
	Zr_2	1	2.74	1	2.76
		1	2.58	1	2.62
	Zr_3	1	2.76	1	2.75
		1	3.36	1	3.30
	Ni_4	1	2.87	1	2.82
		-	--	1	2.67
	Ni_5	1	2.74	-	--
	Ni_6	1	2.81	1	2.74
	Ni_8	1	2.50	1	2.62
Ni_8	Zr_1	1	2.60	1	2.77
		1	2.34	1	2.77
	Zr_3	1	2.79	1	2.83
		1	2.78	1	2.80
		1	2.75	1	2.65
	Ni_4	1	3.07	1	3.08
	Ni_5	1	2.73	1	2.65
	Ni_6	1	2.72	1	2.68
	Ni_7	1	2.50	1	2.62
	Ni_8	1	2.76	1	2.80

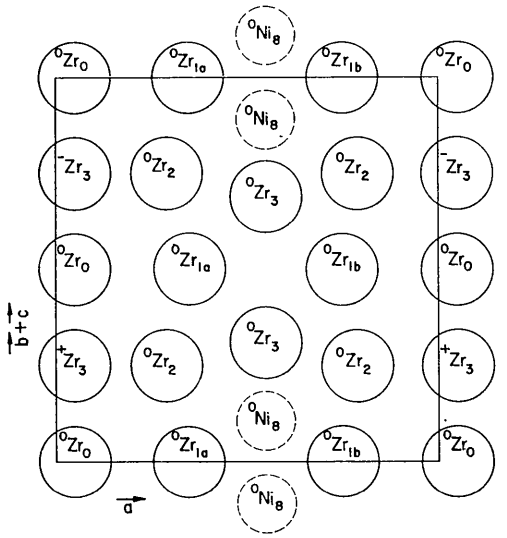

Fig. 4. The atomic arrangement in the zirconium layers is illustrated. The prefixed superscript zero designates atoms which are very nearly coplanar while the prefixed + and − designate atoms which are, respectively, above and below the plane. The lattice parameters, **a**, **b**, and **c**, form a right hand set. If the solid lines represent translations of the unit cell as indicated by the vectors and the lower left corner of the rectangle outlined by these translations is chosen as the origin of the unit cell, then the illustrated layer is the $(01\bar{1})$ plane passing through the center of the unit cell. Successive layers may be reproduced by the *C*-centering symmetry operation which gives rise to four such layers per unit cell. The atomic arrangement in (011) planes is essentially equivalent. This can be illustrated by replacing $\mathbf{b}+\mathbf{c}$ in the figure by $\mathbf{b}-\mathbf{c}$. If, in addition, the origin of the unit cell is placed at $\frac{1}{2}(\mathbf{b}-\mathbf{c})$, the illustrated plane again passes through the center of the unit cell.

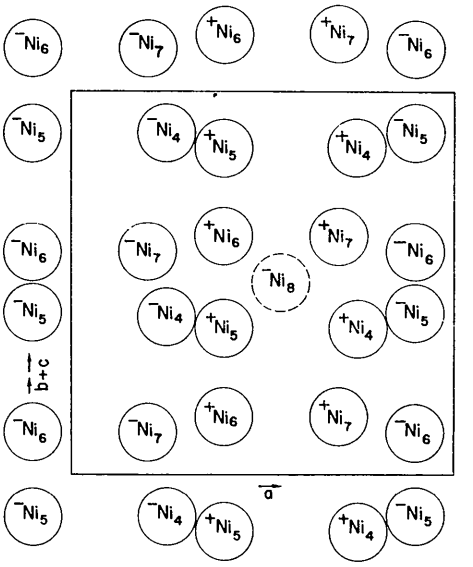

Fig. 5. The atomic arrangement in the nickel layers is shown. Again the prefixed + and − indicate, respectively, atoms above and below the plane. If the rectangle in this figure is superposed over that in Fig. 4, the atomic arrangement will be that of the first nickel layer in the $\mathbf{b}-\mathbf{c}$ direction from the zirconium layer of Fig. 4. This plane as illustrated is in a $(01\bar{1})$ orientation. Note that the Ni_8 atom is located such that it can be shared with an intersecting zirconium plane of (011) orientation.

The zirconium layering in the $Ni_{10}Zr_7$ structure is illustrated in Fig. 4 and the adjacent nickel layering in Fig. 5. The layers are repeated by the $\frac{1}{2}a+\frac{1}{2}b$ translation of the *C*-centering operation (or the equivalent in *Pbca*), and the projective component of the translation normal to the layer is one-quarter of the unit cell translation. Thus every fifth layer duplicates the first. It may also be noted that the Ni_8 atoms in the (011) zirconium planes are shared by the intersecting $(01\bar{1})$ nickel planes; the atomic arrangement which permits this sharing is evident from Fig. 5.

Some inference about the loci of the substitutional replacement of nickel atoms by zirconium atoms may be made from the data in Table 7 with due note of the fact that the zirconium atom is considerably larger than the nickel atom. It is of interest that the interatomic distances about the Ni_4, Ni_5, Ni_6, and Ni_7 atoms are on the average significantly larger for the zirconium-rich composition than for the stoichiometric composition. The inverse is true for the Ni_8 atoms. This would preclude any appreciable substitution of zirconium atoms on the Ni_8 sites and is consistent with the unique position of the Ni_8 atoms in the structure. A further elimination of the Ni_4, Ni_5, Ni_6, or Ni_7 sites as possible zirconium positions does not seem warranted on the basis of the available data. It is doubtful that further refinement of the data to locate the set or sets substituted with zirconium atoms would be fruitful since the substitution of two zirconium atoms among any or all of the four sets changes the effective scattering factors by only a small percentage, and the reliability of the visually estimated intensity data is inadequate to permit establishing the degree of occupancy of each of the four atomic sets. However, the Ni_4 and Ni_5 and also the Ni_6 and Ni_7 sites are crystallographically closely related and indeed a slight shift in positional parameters would place them in sixteenfold sets in D_{2h}^{18}–*Cmca*. It is quite probable, therefore, that the zirconium substitution is approximately random in all four sets. Certainly the dissolution of zirconium results in an increase in symmetry and this must be interpreted to signify that the substitution is random in the sense that there is no long range ordering of the substituted zirconium atoms. The strain distortion resulting from the size difference between zirconium and nickel atoms accounts for the shift in atomic coordinates and bond lengths in the zirconium-rich phase.

References

BUERGER, M. J. (1942). *X-Ray Crystallography*. New York: Wiley.

BUERGER, M. J. (1960). *Crystal-Structure Analysis*. New York: Wiley.

FITZWATER, D. R. (1958). Dissertation for Ph.D. degree, Iowa State University, Ames, Iowa.
FITZWATER, D. R. & WILLIAMS, D. E. (1958). U.S. Atomic Energy Commission, interior Ames Laboratory Report No. AL-140, Ames, Iowa.
KIRKPATRICK, M. E. & LARSEN, W. L. (1961). *Trans. Amer. Soc. Met.* **54**, 580.
KIRKPATRIC, M. E., BAILEY, D. M. & SMITH, J. F. (1962). *Acta Cryst.* **15**, 252.
LU, C. S. (1943). *Rev. Sci. Instrum.* **14**, 331.
NELSON, J. B. & RILEY, D. P. (1945). *Proc. Phys. Soc. Lond.* **57**, 160.
PEARSON, W. B. (1958). *Handbook of Lattice Spacings and Structures of Metals and Alloys*, p. 95. New York: Pergamon.
SMITH, E. & GUARD, R. W. (1957). *J. Metals*, **9**, 1189.
THOMAS, L. H. & UMEDA, K. (1957). *J. Chem. Phys.* **26**, 293.
ZALKIN, A. & JONES, R. E. (1956). *Incor I Program for Single Crystal X-ray Diffraction Data*. University of California Radiation Laboratory, Berkeley, California.

Acta Cryst. (1962). **15**, 903

The Crystal Structure of α-Niobium Tetraiodide

BY LAWRENCE F. DAHL AND DALE L. WAMPLER*

Department of Chemistry, University of Wisconsin, Madison 6, Wisconsin, U.S.A.

(*Received* 30 *October* 1961 *and in revised form* 26 *December* 1961)

Crystals of α-NbI_4 are orthorhombic, space group $Cmc2_1$, lattice parameters

$$a = 7{\cdot}67 \pm 0{\cdot}02,\ b = 13{\cdot}23 \pm 0{\cdot}02,\ c = 13{\cdot}93 \pm 0{\cdot}02\ \text{Å},$$

with eight formula units in the unit cell. Final refinement by a three-dimensional anisotropic least-squares analysis resulted in an R value of 8·6%.

The structure of solid α-NbI_4 is based on a distorted hexagonal close-packing of the iodine atoms. One-fourth of the available octahedral holes are occupied by niobium atoms to give infinite linear chains formed by NbI_6 octahedra sharing opposite edges. The niobium atoms are shifted from the centers of the octahedra toward one another in pairs to give a resulting Nb–Nb distance of 3·31 Å. Weak metal–metal interactions which couple the unpaired electrons completely explain these niobium shifts and account for the observed diamagnetism of α-NbI_4. The valency state of niobium in α-NbI_4 is concluded to be IV from the observed identical environments of the niobium atoms. α-NbI_4 and the isomorphous TaI_4 are the first simple metal halides which have this structure.

Introduction

Corbett & Seabaugh (1958; Seabaugh, 1961) have synthesized and characterized by both chemical and physical means a number of new niobium iodide compounds including NbI_5, NbI_3, Nb_3I_8, and two different forms of NbI_4 (α-NbI_4 and β-NbI_4).

Complete characterization by single-crystal X-ray diffraction is needed to reveal intimate structural interrelationships among these compounds as well as to provide important fundamental knowledge concerning their nature of bonding. This investigation of the low-temperature form of NbI_4, α-NbI_4, was undertaken with the additional object of establishing the valency state of niobium in the compound. Normally tetravalent niobium should possess an unpaired electron and hence be paramagnetic.†

Rolsten (1958) prepared the presumably isomorphous TaI_4 and found it to be diamagnetic. He speculated that the unpaired electron in TaI_4 must be paired by formation of a dimer or else solid TaI_4 must exist in a mixed oxidation state as Ta(III)Ta(V)I_8. Mixed oxidation states (i.e., I and III) have been found for gallium and for indium dihalides (Corbett & McMullan, 1955, 1956; McMullan & Corbett, 1958; Woodward *et al.*, 1956; Garton & Powell, 1957; Corbett & Hershaft, 1958; Carlston *et al.*, 1958; Clark *et al.*, 1958).

Brauer (1948) reported NbO_2 to be weakly paramagnetic although much less than expected for Nb(IV) ions. Schäfer *et al.* (1961) found $TaOCl_2$ and the tantalum and niobium tetrahalides (X = Cl, Br, and I) to be diamagnetic and consequently suggested the presence of similar bonding conditions in niobium and tantalum compounds of the general type MX_4, MOX_2, and MO_2. They also stated that no isolated Ta(IV) ions are present in $TaOCl_2$ but did not comment further on the valency state in these compounds. The structural determination of α-NbI_4 revealed weak metal–metal bonding and thereby explained

* National Science Foundation Predoctoral Research Fellow, 1959–61. Present address: Dept. of Chemistry, Juniata College, Huntingdon, Pennsylvania, U.S.A.

† α-NbI_4 initially was reported to be paramagnetic (Corbett & Seabaugh, 1958), but in view of our structural results a redetermination of the magnetic susceptibility by Corbett & Seabaugh (1959) showed the compound to be diamagnetic.